Radiation Physics and Chemistry 155 (2019) 150–157

Contents lists available at ScienceDirect

Radiation Physics and Chemistry

journal homepage: www.elsevier.com/locate/radphyschem

Thermoluminescence and optically stimulated luminescence of $PbO–H_3BO_3$ and $PbO–H_3BO_3–Al_2O_3$ glasses

G.R. Barrera[a,b], L.F. Souza[c], A.L.F. Novais[a,d], L.V.E. Caldas[c], C.M. Abreu[a], R. Machado[a], E.M. Sussuchi[e], D.N. Souza[a,*]

[a] Universidade Federal de Sergipe, Departamento de Física, Av. Marechal Rondon, s/n, 49100-00 São Cristóvão, SE, Brazil
[b] Corporación Universitaria del Huila, Calle 21 No. 6 - 01/Prado Alto: Calle 8 No. 32–49 Huila, Colombia
[c] Instituto de Pesquisas Energéticas e Nucleares, Comissão Nacional de Energia Nuclear, IPEN/CNEN-SP, Av. Prof. Lineu Prestes 2242, 05508-000 São Paulo, SP, Brazil
[d] Universidade Federal do Sul e Sudeste do Pará, Folha 31, Quadra 07, Lote Especial, s/n., 68507-590 Nova Marabá – Marabá, PA, Brazil
[e] Universidade Federal de Sergipe, Departamento de Química, Av. Marechal Rondon, s/n, 49100-00 São Cristóvão, SE, Brazil

A B S T R A C T

In the present work some dosimetric and structural properties of the lead borate glass ($4.5PbO\text{-}1.9H_3BO_3$) and lead aluminum borate glass ($11.1PbO\text{-}2.9H_3BO_3\text{-}0.2Al_2O_3$) were investigated. The glass samples were produced by fusion and fast cooling method. The dosimetric characterization was performed via thermoluminescence (TL) and optically stimulated luminescence (OSL) techniques. For this characterization, the samples were irradiated with a beta source ($^{90}Sr/^{90}Y$). TL emission curves, kinetic parameters, OSL decay curves, dose response curves, and the correlation between TL and OSL results were obtained. X-ray diffractometry (XRD) and infrared spectroscopy (FT-IR) of the samples were also performed. The XRD analyses confirmed the amorphous nature of the investigated glasses and the FT-IR analyses showed the different borate groups in their compositions. The TL emission curves of the glasses are composed by three peaks, located at different temperatures. The dose response curve in both TL and OSL analyses indicated linearity for most of the dose range studied. The OSL decay curves exhibited two components with different decay times.

1. Introduction

Borate glasses have been widely investigated due to their variety of technological applications, such as in optics, electronics, biomedical and radiation dosimetry. This variety of fields of applications is associated with the excellent transparency characteristics in both visible and infrared regions, and because they can be produced over a wide range of composition (Chung, 2010; Marini et al., 2015).

The application of borate glasses has been prominent in ionizing radiation dosimetry through luminescent techniques such as thermoluminescence (TL), optically stimulated luminescence (OSL) and radiophotoluminescence (RPL) (Chung, 2010; Hsu et al., 2008; Yukihara and Mckeever, 2011). The luminescent dosimetry is a well-established and commercially available technique for already more than four decades (Mckeever, 1985; Mckeever and Yukihara, 2008; Mckeever et al., 1995; Bhatt and Kulkarni, 2013). Some examples of most used thermoluminescent dosimeters (TLD) are LiF:Mg,Ti, CaF:Mn, $CaSO_4$:Dy, $Li_2B_4O_7$, and the aluminophosphate glasses that are used for OSL and RPL dosimetry (Hsu et al., 2008; Mckeever and Yukihara, 2008; Bhatt and Kulkarni, 2013; Mckeever and Chen, 1997; Akselrod et al., 2007).

Nowadays there is a strong tendency to substitute the TL for the OSL technique, due to the optical nature of the measurement process, the controlled stimulus form, the rapid readings (few seconds) and the possibility of re-reading the signal to re-estimating of absorbed doses (Yoshimura and Yukihara, 2006). However, because it is a relatively recent technique, there are only few commercial OSL dosimeters available, the Al_2O_3:C commercialized by Landauer Inc. (Yukihara and Mckeever, 2011; Mckeever and Yukihara, 2008; Ahmed et al., 2014; Akselrod and Akselrod, 2006) and BeO are the only synthetic materials used (Yukihara and Mckeever, 2011).

Although Al_2O_3:C is extremely sensitive to the OSL technique, it has inherent limitations, such as: low neutron cross section, high effective atomic number (Z_{eff} = 11.28), and its high lifetime of emission of the F center (35 ms) is an obstacle for 2D dose mapping (Akselrod and Akselrod, 2006; Yukihara et al., 2017). BeO is very sensitive to radiation, and has Z_{eff} = 7.6, comparable to the soft tissue, but in the powder form it presents high toxicity, consequently limiting its applicability to

* Corresponding author.
E-mail address: divanizi@ufs.br (D.N. Souza).

https://doi.org/10.1016/j.radphyschem.2018.02.005
Received 31 July 2017; Received in revised form 23 January 2018; Accepted 5 February 2018
Available online 08 February 2018
0969-806X/

the form of chips, cylinders and rigid plates (Yukihara et al., 2017; Souza et al., 2015). Thus, many research groups have focused on the development of materials with a luminescent efficiency similar to the reference TL and OSL dosimeters, and which bring new solutions to different dosimetry practices such as in vivo dosimetry (Ahmed et al., 2014; Yukihara et al., 2017).

The use of vitreous matrices has been a notable alternative in TL, OSL and RPL dosimetry, since such matrices present advantages, including optical transparency (which improves the luminescent efficiency of the material) relatively simple and low-cost production process, structural rigidity and high chemical durability (Yutaka et al., 2014; Hirao et al., 2001; Justus et al., 1995; Teixeira et al., 2008). Therefore, the investigation and improvement of vitreous systems for luminescent dosimetry practices have been assiduously described in the literature (Marini et al., 2015; El-Adawy et al., 2010; Rao et al., 2013; Doweidar et al., 2012). In addition, glasses containing heavy metal oxides (HMO), for example Pb, Cd and Bi, are known to exhibit low phonon energies, high refractive indices, low transition temperature, high polarizability and good rare-earth ions solubility that significantly increases the optical and electronic properties (Hsu et al., 2008; Rao et al., 2013; Doweidar et al., 2012).

In the present work, the suitability of $PbO:H_3BO_3$ and $PbO:H_3BO_3–Al_2O_3$ glasses will be presented for radiation dosimetry applications using TL and OSL techniques.

Some important TL parameters such as TL emission curves and dose response curves were obtained; the trap parameters (kinetic parameters) of TL glow curves were defined through the peak shape method and the curve fitting method (Chen and Mckeever, 1997). The OSL decay curves, the dose response for OSL and the correlation between TL and OSL signals from the glasses were also investigated.

The OSL and TL phenomena are correlated, except in the case of TL where the stimulation of the trapped charge that ultimately leads to recombination and luminescence is due to thermal energy, provided to the crystal by heating (Yukihara and Mckeever, 2011). This correlation is very important from the theoretical point of view to identify how deep, with respect to the conduction band, trapping centers are those that contribute to the OSL signal. This information helps for the understanding of the influence of other trapping centers (e.g., shallow traps or deeper traps) on the OSL.

The monitoring of the optical bleaching effects on the TL curves can provide useful insight into the OSL process. It is possible to investigate which TL peaks are affected by optical stimulation through the comparison between the TL curves obtained immediately after irradiation of the material and those obtained after irradiation and optical stimulation (bleaching). Using this method, it can be seen if the traps responsible for the TL emission are the same ones responsible for the OSL signal of the material.

A greater understanding and description of the glass matrix structure should promote an improvement in the quality of the glasses as dosimeters; therefore, this work also brings results of structural and optical characterization of the glasses, which were analyzed using X-ray diffractometry (XRD) and infrared spectroscopy (FT-IR).

2. Materials and methods

2.1. Glass and pellet preparation

The glasses were synthesized through the fusion and fast cooling methods using the following raw materials: lead monoxide (PbO), boric acid (H_3BO_3), and aluminum oxide (Al_2O_3). All of the compounds are from Sigma Aldrich, with 99.99% degree of purity. The lead borate ($4.5PbO\text{-}1.9H_3BO_3$) samples were produced with stoichiometric percentages, considering weight (wt%), of 70.31 for PbO and 29.66 for H_3BO_3. The aluminum borate ($11.1PbO\text{-}2.9H_3BO_3\text{-}0.2Al_2O_3$) samples were obtained with 78.16, 20.42 and 1.42 of wt% for the PbO, H_3BO_3 and Al_2O_3, respectively.

The compounds were mixed in porcelain crucibles at room temperature and heated at 550 °C for 2 h for thermal decomposition of the sodium carbonate and decomposing the boric acid. Thereafter, the temperature was raised to 800 °C and the mixtures were held at this temperature for two hours. Subsequently, the temperature was further increased to 1100 °C and held for 0.5 h. The obtained glass samples were quenched by pouring the molten glass onto an alumina crucible.

Pellets were produced with the glass samples for TL and OSL studies. For the pellets production, some pieces of glass were grounded and those powdered samples with grain size between 75 and 180 μm were selected. For each material, a set of 20 pellets was produced using Teflon as the agglutinator, with mass proportion of 1 (glass):0.4 (Teflon). Each pellet has a mass of (50.0 ± 0.1) mg, with 6.0 mm diameter and 2.0 mm thickness. For the sintering process, the samples were thermally treated sequentially at 300 °C for 30 min and 400 °C for 1.5 h in a furnace (EDG-1800, USA).

2.2. Experimental methods

2.2.1. X-ray diffractometry

The amorphous structures of the samples were confirmed by X-ray diffractometry in a Rigaku DMAX 2000 CuKα model. The XRD analyses were performed with the tube operating at 40 kV/20 mA with steps of 2θ (deg) = 0.5 in the 2θ scan range from 10° to 80°, with 10 s per step, at room temperature. For these analyses, grain sizes of less than 75 mm were used.

2.2.2. Infrared spectroscopy

Local structure of lead borate and lead aluminum borate glasses were studied by the FT-IR spectroscopy technique. The spectra were obtained in the range of 4000–400 cm^{-1} at room temperature in a Varian 640 spectrometer (typical resolution of 4 cm^{-1} and 64 accumulations). The samples were in the form of disc shape pellets.

2.3. TL/OSL analyses and irradiations

A Risø reader system was used for the TL/OSL analyses and irradiations. The system is equipped with a $^{90}Sr/^{90}Y$ beta source for irradiation, delivering 0.1 Gy/min at the sample position, and a photomultiplier tube (PMT) for light detection (model 9235QB, Electron Tubes, Inc., Middlesex, UK). TL measurements were performed using a continuous ramp until 500 °C, with a heating rate of 5 °C s^{-1}, in nitrogen atmosphere. The detection filter used was a BG-39 (6 mm total thickness, Schott AG, Mainz, Germany, transmission between 330 and 620 nm). The OSL readouts were carried out in the Risø system using the continuous-wave (CW) mode, with blue light stimulation (centered at 470 nm, irradiance of 30 mW/cm) from LEDs.

TL and OSL procedures were performed using five pellets for each kind of glass. For both TL and OSL analyses a maximum standard deviation of 5.5% was obtained. For the OSL bleaching procedure, the pellets were irradiated with 5 Gy from the beta source, and then they were optically stimulated for 80 s with blue light, and finally the TL emission was recorded with a heating rate of 5 °C s^{-1}.

For the determination of kinetic parameters, the peak shape method (PSM) and the curve fitting method (CFM), proposed by Chen and McKeever (Chen and Mckeever, 1997), were used to determine the following parameters: kinetic order (b), activation energy (E) and frequency factor (s). The stability of the emission peak TL is directly related to the activation energy, also called trap depth in the band gap of the material (Yukihara and Mckeever, 2011; Mckeever and Yukihara, 2008; Mckeever et al., 1995). Indeed, the application of the PSM is based on the Chen's equations (Chen and Mckeever, 1997; Horowitz, 1984; Kitis et al., 2000). The PSM method has been applied to the experimental glow curves. The expressions deduced by Chen, valid for any kinetic order, are described here as presented at (Kitis et al., 2000):

$$E_\gamma = C_\gamma\left(\frac{kT_m^2}{\gamma}\right) - b_\gamma(2kT_m) \quad (1)$$

where γ stands for τ, δ and ω; in which $\tau = T_m - T_1$, $\delta = T_2 - T_m$, and $\omega = T_2 - T_1$. T_m is the temperature at the maximum of the glow peak, and T_1 and T_2 are the temperatures at half of the maximum intensity, on the ascending and descending parts of the TL peak, respectively. The Boltzmann constant is represented by k. The values of C_γ and b_γ depend on which of these three parameters of the peak is used. When the ascending part of the peak is used, the previous quantities become:

$$C_\tau = 1.15 + 3(\mu_g - 0.42) \quad (2)$$

$$b_\tau = 1.58 + 4.2(\mu_g - 0.42) \quad (3)$$

When the descending part is taken into consideration:

$$C_\delta = 0.976 + 7.3(\mu_g - 0.42); b_\delta = 0 \quad (4)$$

When the full width at half maximum (FWHM) is used:

$$C_\omega = 2.52 + 10.2(\mu_g - 0.42); b_\omega = 1 \quad (5)$$

In these expressions $\mu_g = \delta/\omega$ is named as geometrical factor. Chen also provided a plot which allows one to obtain the kinetic order of the process, according to the value of the geometrical factor. The TL peaks that obey the first order kinetic present $\mu_g = 0.42$, and those who obey the second-order kinetic present $\mu_g = 0.52$. In most of the cases, the peaks present intermediate kinetics, and it is represented by $0.42 < b < 0.52$. The frequency factor (s) was calculated through the following equation:

$$\frac{\beta E}{kT_m^2} = s\left[1 + (b-1)\frac{2kT_m}{E}\right]exp\left(\frac{-E}{kT_m}\right) \quad (6)$$

where β is the given heating rate.

Physically, the frequency factor represents the number of oscillations that the electron executes per second in the traps (Horowitz, 1984; Kitis et al., 2000).

The CFM defines the parameters E, s and b, from the TL emission curve, through numerical computation based on a specific model and considering certain initial approximation from the values of parameters in the equation. Thus, a theoretical curve is generated based on the kinetic model for the first order (b = 1), or at a general order, with b ≠ 1. The theoretical curve is generated and compared with the experimental curve and the deviation between them is calculated. The procedure is continued varying E, s e b until the minimum deviation is found. The calculated parameter values for a given minimum deviation represent the values of the TL parameters that best fit the theoretical curve (Chen and Mckeever, 1997). All the data processing was done using the *OriginLab 8.0* software. The dose response curves, for TL and OSL, were fitted using a polynomial cubic equation (Eq. (7)):

$$y(D) = K_0 + K_1D + K_2D^2 + K_3D^3 \quad (7)$$

where K_1, K_2 and K_3 are constants and D is the absorbed dose. The dose response curves were plotted using this equation. A quantitative analysis of the superlinearity index of the dose response for TL and OSL glow curves was performed, showing a more realistic vision of how the slope of the dose response curve changes for different doses. The superlinearity index is described by the following equation (Chen and Mckeever, 1997):

$$g(D) = \left[\frac{Dy''(D)}{y'(D)}\right] + 1 \quad (8)$$

where y(D) is the polynomial cubic equation created for each dose response curve, y′(D) and y″(D) are the first and second derivatives of the function y(D). g (D) is dimensionless; g (D) > 1 indicates a supralinear response, while g (D) = 1 means a linear response, and if g(D) < 1 a sublinear behavior is observed.

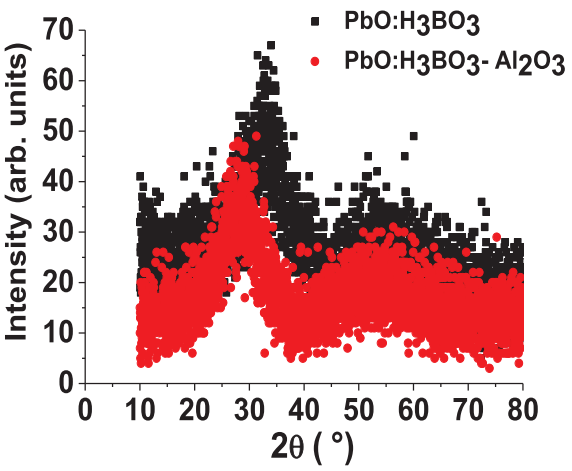

Fig. 1. XRD patterns of the PbO:H_3BO_3 and PbO:H_3BO_3-Al_2O_3 glasses.

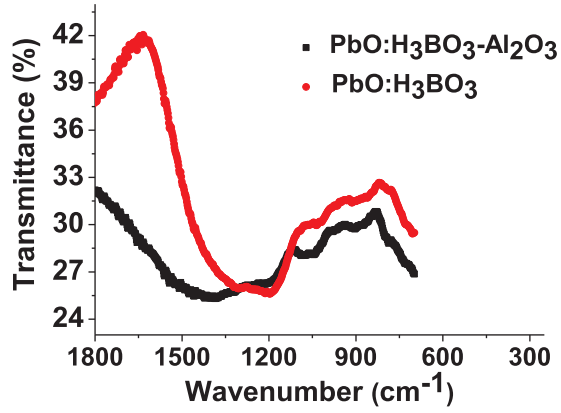

Fig. 2. FT-IR of the PbO:H_3BO_3-Al_2O_3 and PbO:H_3BO_3 glasses.

3. Results and discussion

3.1. X-ray diffractometry

Glasses are amorphous materials that have no crystalline periodicity and thus do not possess diffraction patterns with sharp peaks as observed in crystalline materials (Dayanand, 2004; Cheng et al., 2007; Boulos and Kreidl, 1971; Singh et al., 2004).

Fig. 1 shows that the X-ray diffraction patterns of PbO:H_3BO_3-Al_2O_3 and PbO:H_3BO_3 are composed by broad bands peaks, which ensure the amorphous nature of these samples. This behavior corroborates with the formation of the vitreous structures.

Although the XRD patterns from both materials are very similar, a displacement of ± 4° (12%) in the first broadband peak (20° < 2θ < 40°) is observed. Most probably this angular shift observed between these two materials is due to the distribution of the powder sample on the sample holder made of a transparent glass, where the powder is accommodated in the center. The most delicate part of this process is how the powder is distributed in the center of the holder, with an appropriate quantity, to make the process as most accurate as possible. To this, sieves with apertures lower than 75 μm were used, which help to distribute the powder homogenously on the sample holder. However, variances between measures are inevitable, which origin this shifting in the intensities on XRD patterns. The quantity of powder placed in the holder can also explain the 25% of relative difference in the intensity observed for these first XRD peaks.

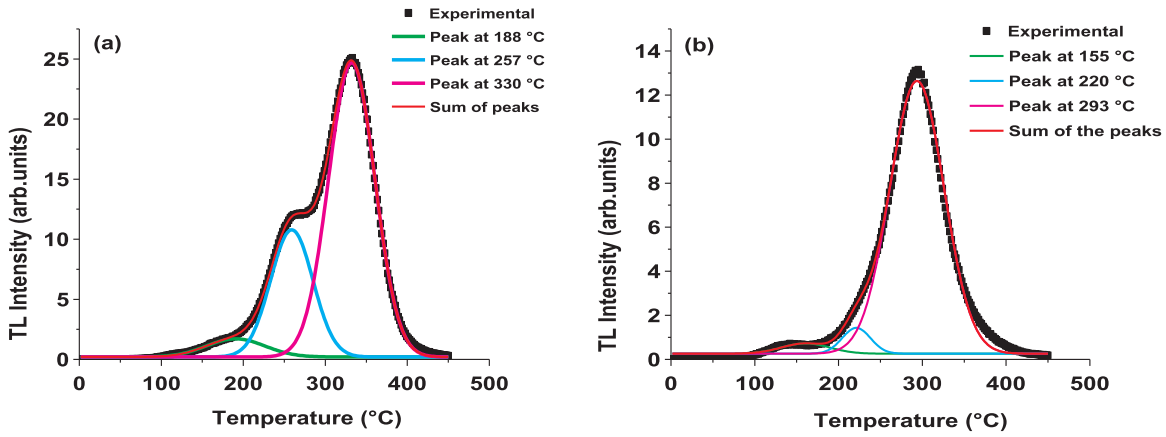

Fig. 3. Decomposition of TL glow curve from the glasses (a) PbO:H_3BO_3 and (b) PbO:H_3BO_3-Al_2O_3 into Gaussian peaks.

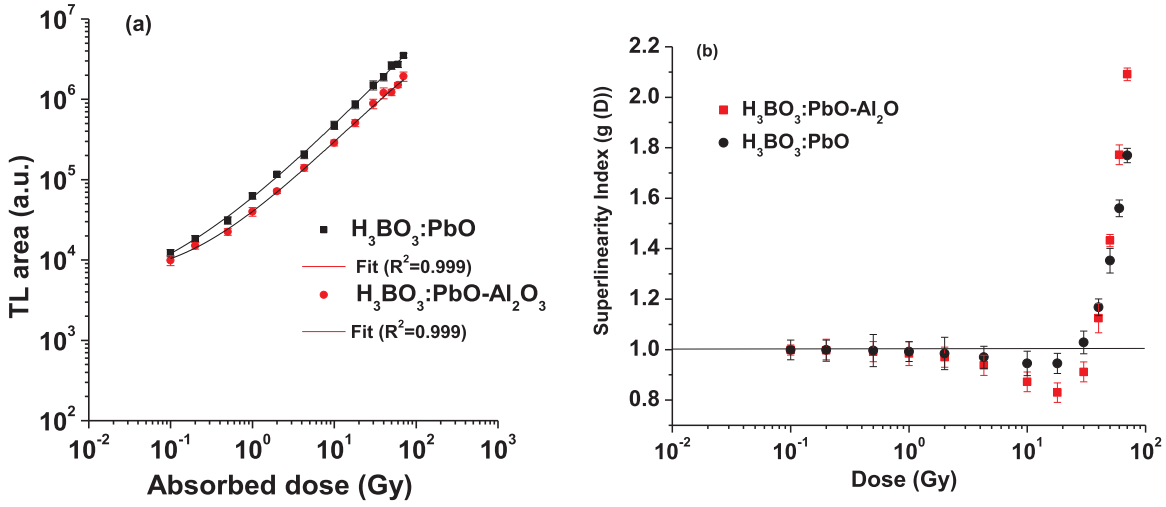

Fig. 4. (a) TL dose response from the glass samples. (b) Superlinearity index g(D) of dose response curves.

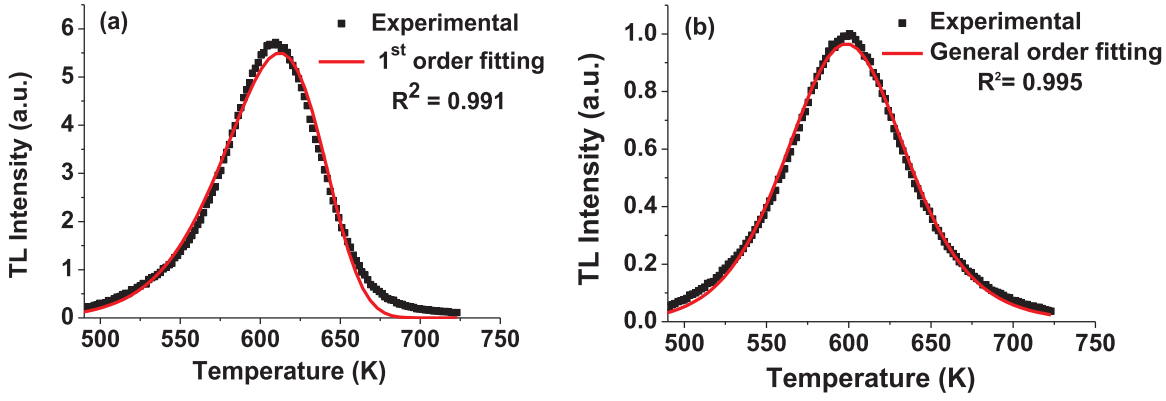

Fig. 5. Curve fitting method for TL emission peak at 330 °C (603 K) for PbO:H_3BO_3. (a) First order fitting; (b) General kinetic order fitting.

3.2. Infrared spectroscopy

In Fig. 2 all of the FT-IR spectra show broad intense bands in the region between 702 and 1200 cm^{-1} and from 1200 to 1400 cm^{-1}. Both spectra present a smooth absorption band, which is very characteristic for borate glasses. Bands in the region 702–1200 cm^{-1} are commonly related to B–O stretching vibration of BO_4 units in various borate groups, like pentaborate, triborate and diborate groups (Cheng et al., 2007; Boulos and Kreidl, 1971; Singh et al., 2004). The absorption bands in the region ~ 1200 to 1400 cm^{-1} are related to the vibration of boron–oxygen rings (Cheng et al., 2007). The intense broad band from 1300 to 1800 cm^{-1} observed at PbO:H_3BO_3-Al_2O_3 is solely related to the B–O stretching vibration of trigonal BO_3 units; these groups are not seen in the PbO:H_3BO_3. The BO_3 units are incorporated in borate groups containing non-bridging oxygen ions, such as metaborate, pyroborate and orthoborate groups (Boulos and Kreidl, 1971).

3.2.1. TL and OSL analyses

Fig. 3(a) shows a typical TL emission glow curve of PbO:H_3BO_3 and the decomposition of the TL curve in three Gaussians peaking at 188 °C,

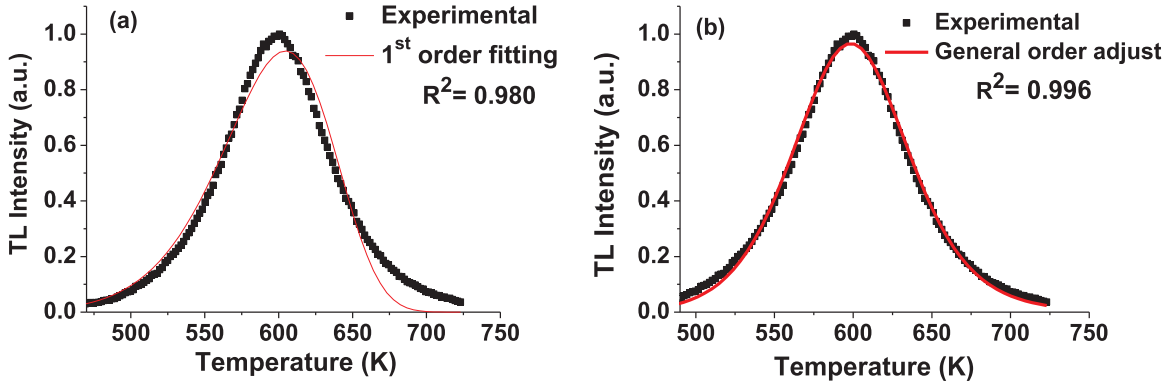

Fig. 6. Curve fitting method for TL emission peak at 326 °C (599 K) for PbO: H_3BO_3-Al_2O_3 (a) First order fitting; (b) General kinetic order fitting.

Table 1
Kinetic parameters (b, E e s) of the TL peak from PbO: H_3BO_3 and PbO: H_3BO_3-Al_2O_3 glass systems, calculated by PSM and CFM methods.

Glass	Method	b	E (eV)	s (s^{-1})
PbO:H_3BO_3	PSM	1.50 ± 0.03	1.26 ± 0.03	(5.94 ± 0.09) × 10^9
	CFM (General order) R^2 = 0.995	1.30 ± 0.02	1.15 ± 0.01	(5.92 ± 0.05) × 10^8
PbO:H_3BO_3-Al_2O_3	PSM	1.70 ± 0.05	1.14 ± 0.03	(8.23 ± 0.07) × 10^9
	CFM (General order) R^2 = 0.996	1.68 ± 0.04	1.06 ± 0.05	(1.33 ± 0.06) × 10^8

257 °C and 330 °C, approximately. For PbO:H_3BO_3-Al_2O_3, the glow curve was also decomposed in three Gaussian peaks, which present maximum intensities at 155 °C, 220 °C and 293 °C. For this analysis, the pellets were irradiated with 10 Gy, and TL emission was recorded. For dosimetric applications it is simpler when the TL glow curve has only one peak, but this is almost impossible for crystalline or glass insulators, once that these materials are composed by different levels of traps and recombination centers that originate different TL emission peaks (Bos, 2001). The most stable peaks are the high temperature peaks (> 200 °C), and they are called dosimetric peaks, because they are less likely to undergo high fading over time, unlike the other peaks located below 200 °C which are known to decay rapidly, a characteristic known as high fading (Pagonis et al., 2006). The dosimetric peaks chosen for the glasses are located at 330 °C for PbO:H_3BO_3 and at 293 °C for PbO:H_3BO_3-Al_2O_3.

The dose response of both glasses was obtained through the integration area of the main TL peak at 330 °C for PbO:H_3BO_3 and at 293 °C for PbO:H_3BO_3-Al_2O_3, and the results are illustrated in Fig. 4.

The fitting applied for the dose response curves was a polynomial cubic function described by Eq. (7). Using this equation, it was possible to obtain a chi-square value of 0.990 for both fittings, which ensure that this equation is suitable for the present quantitative analyses. Using Eq. (8) it is possible to see how exactly the slope of the dose response curves change with the increase of the absorbed dose. The superlinearity index g(D) is shown in Fig. 4. (b). It is possible to see that both glasses present a similar behavior with regions of linear, sublinear and supralinear responses. From 0.1 to 2 Gy a linear response (g (D) = 1) can be observed for both materials; between 2 and 20 Gy, the response is sublinear for PbO:H_3BO_3, and from 2 to 30 Gy the response for PbO:H_3BO_3-Al_2O_3 is sublinear (g (D) < 1). For PbO:H_3BO_3, the response is supralinear for absorbed doses higher than 30 Gy, and for PbO:H_3BO_3-Al_2O, the supralinearity is evidenced above 40 Gy (g (D) < 1).

The deviations from linearity are predicted to occur because of the dynamics of the process of charge capture among the different defects in the materials (Mckeever, 1985; Mckeever et al., 1995; Mckeever and Chen, 1997). The physical phenomena that cause the occurrence of supralinear regions in TL dose response are associated to competitive processes of trapping centers during the irradiation and heating of the materials (Bos, 2001).

The kinetic parameters quantitatively describing the trapping–emitting centers responsible for the TL emission of the glasses are shown in Figs. 5 and 6 and in Table 1. For the PbO:H_3BO_3 [Fig. 5], the best fitting is for the general kinetic order that is represented by b = (1.30 ± 0.02) when calculating by CFM. The E and *s* values for this material, obtained through this method, were (1.15 ± 0.01) eV and 5.9 × 10^8 s^{-1}, respectively.

For PbO:H_3BO_3-Al_2O_3, the fitting for the first and second kinetic

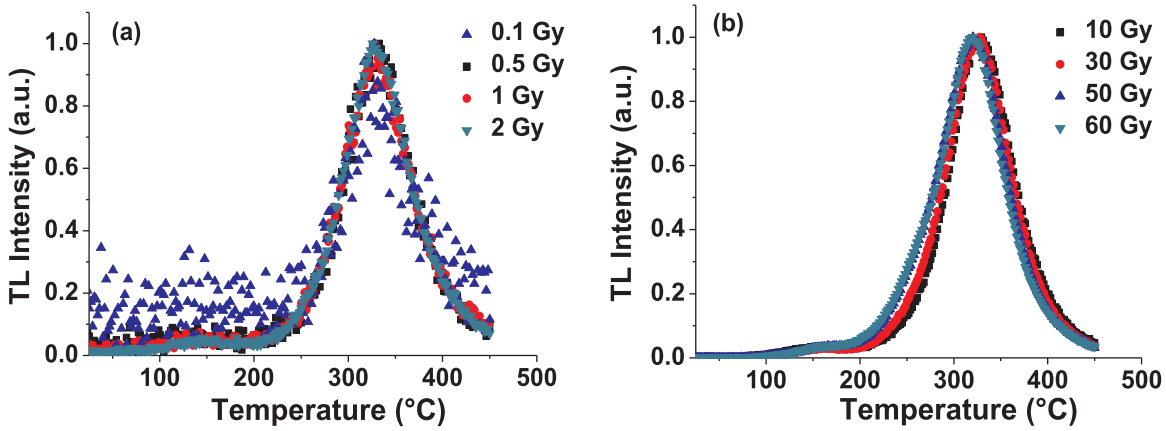

Fig. 7. TL glow curves of PbO:H_3BO_3-Al_2O_3 irradiated with absorbed doses in the range (a) 0.1–2 Gy, and (b) 10–60 Gy.

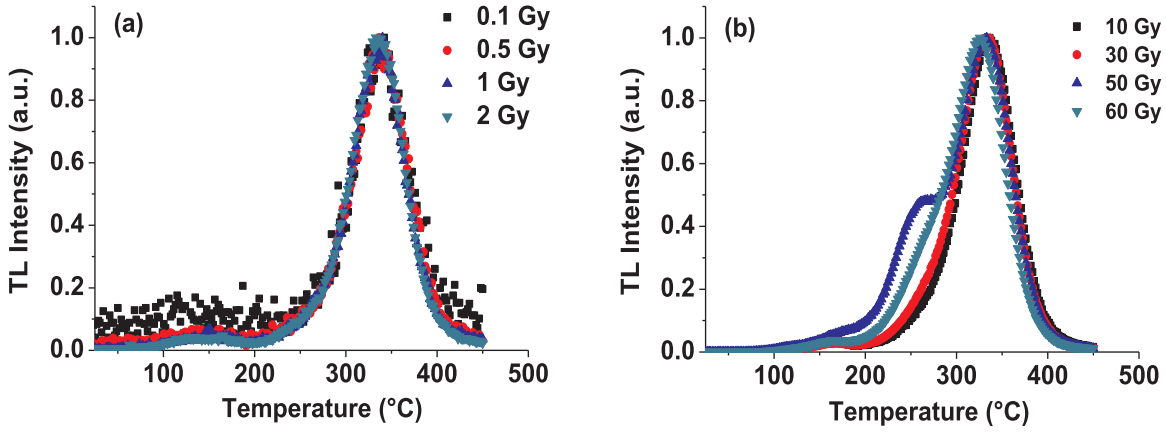

Fig. 8. Normalized TL glow curves of PbO:H_3BO_3 irradiated with absorbed doses in the range: (a) 0.1–2 Gy and (b) 10–60 Gy.

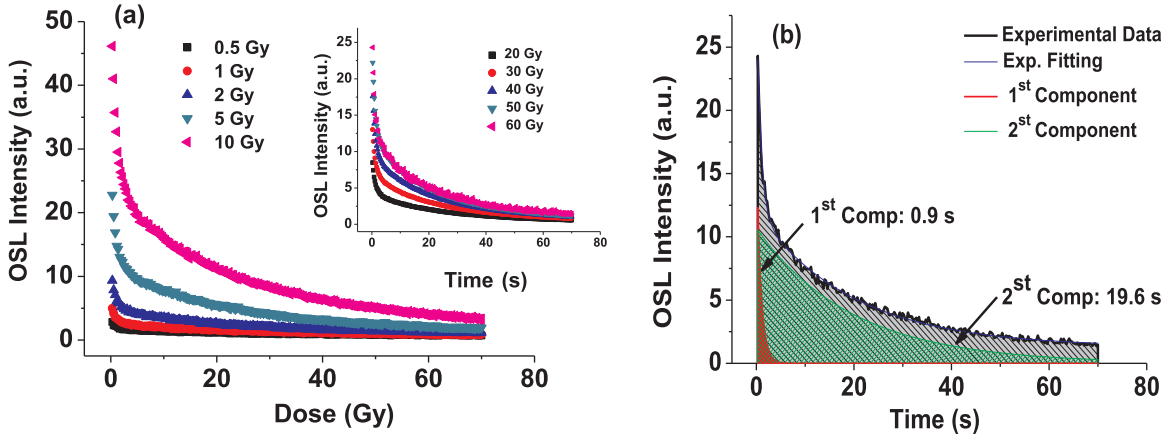

Fig. 9. (a) OSL decay curves of PbO:H_3BO_3 samples irradiated with absorbed doses in the range 0.5–60 Gy. (b) The fitting of the OSL decay curve and the contribution of the fast and slow components is shown in the filled area.

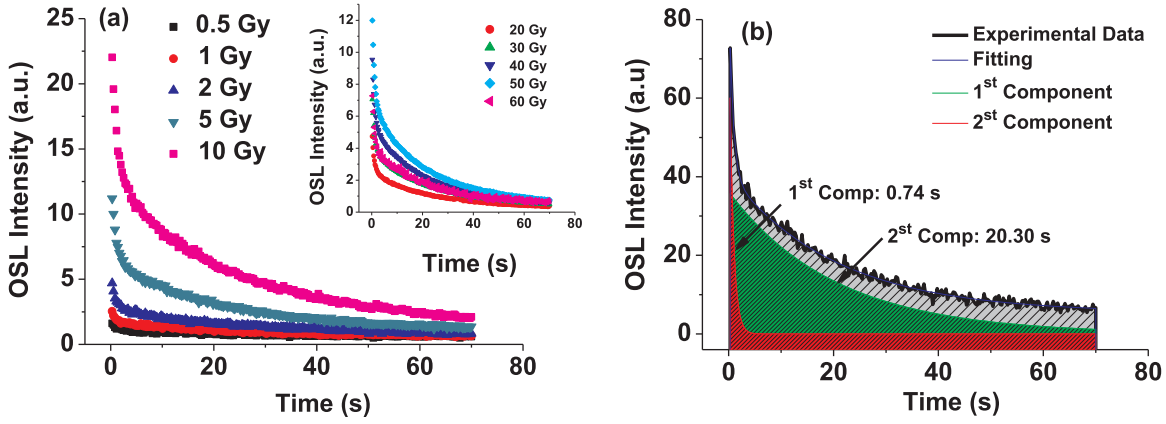

Fig. 10. (a) OSL decay curves of the PbO:H_3BO_3-Al_2O_3 samples irradiated with absorbed doses in the range 0.5–60 Gy. (b) The fitting of the OSL decay curve and the contribution of the fast and slow components is shown in the filled area.

order TL peak around 293 °C is shown in Fig. 6(a) and (b). The best fitting is for general order as well, with b, E and s values of (1.68 ± 0.02); (1.06 ± 0.01) eV and (1.33 ± 0.06) × 10^8 s^{-1}, respectively. The kinetic parameters of the glasses obtained through PSM are presented in Table 1 where they are compared with those obtained using the CFM method.

It is important to note that there is a good agreement between CFM and PSM values of kinetic parameters for the TL emission of both glasses. The *b* values for both glasses do not fit neither first nor the second–kinetic order, but they are consistent with the TL peaks of general kinetic order. Although the TL emission curves of the samples did not strictly follow the first or the second kinetic order cases, a very important observation is that the maximum position and the shape of TL peak (293 °C) for PbO:H_3BO_3-Al_2O_3 [Fig. 7] did not vary with the dose. This is a very positive characteristic for use of this glass in dosimetric purposes, once the absorbed dose is proportional to the area under of TL curve, and any change in the position or in the shape of TL curve can add errors to the dose estimative (Bos, 2001). This observation is not true for the PbO:H_3BO_3 glass, because for higher doses (above 50 Gy), the glow curve shape starts to alter, and it is observed

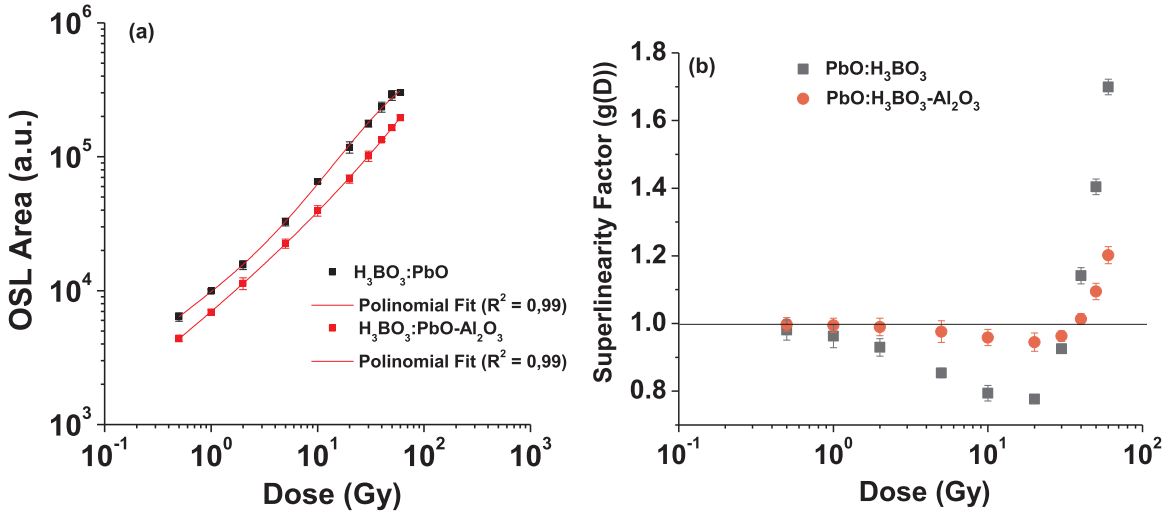

Fig. 11. (a) OSL dose response curves for $PbO:H_3BO_3$-Al_2O_3. (b) Superlinearity index g(D) of OSL dose response curves.

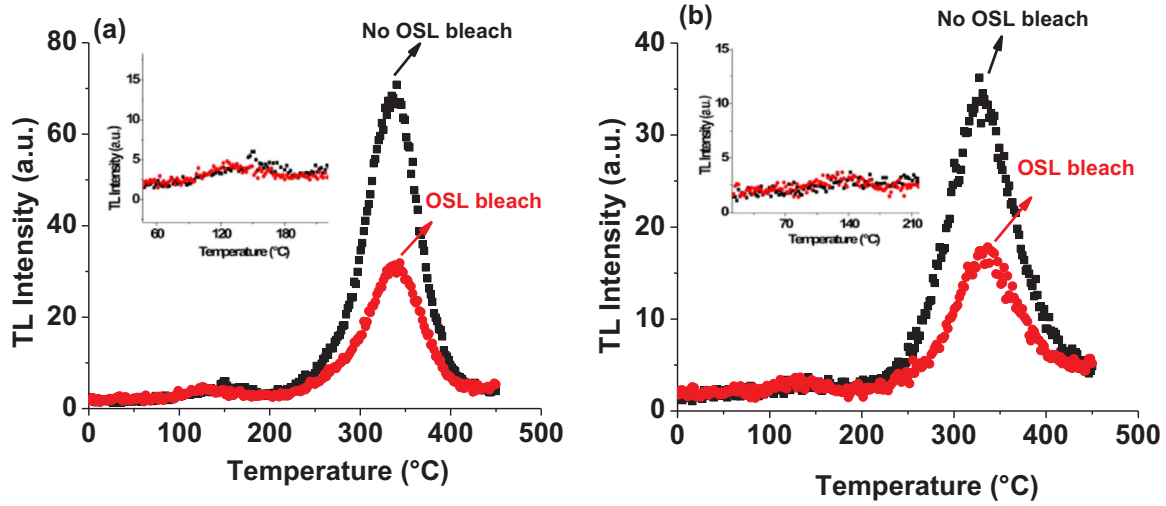

Fig. 12. Comparison between TL signals of $PbO:H_3BO_3$ (a) and $PbO:H_3BO_3$ -Al_2O_3 (b) before and after OSL readout during 80 s.

that a small satellite peak appears around 257 °C [Fig. 8]. Physically, the small satellite peak around 257 °C from $PbO:H_3BO_3$-Al_2O_3 is possibly due to radiation-induced defect states in bulk samples (Yukihara et al., 2004; Rao et al., 2014).

Higher values of activation energies (E) were obtained for the $PbO:H_3BO_3$ samples, which means that the traps responsible for the luminescent emission in these host matrices are located in deeper positions in the band gap in comparison to the traps of the $PbO:H_3BO_3$-Al_2O_3 samples.

3.2.2. OSL analysis

Figs. 9(a) and 10(a) show the OSL curves of $PbO:H_3BO_3$ and $PbO:H_3BO_3$-Al_2O_3 vitreous samples, respectively irradiated with different doses. As expected, there is an increase in OSL intensity as a function of the dose due to the greatest number of trapped charges. The increase of radiation dose causes both to increase of the initial intensity and integral OSL curves. The OSL decay curves of both samples are well fitted by a double exponential decay described in Eq. (9):

$$I = I_0 + A_1 e^{\left(\frac{-x}{\tau 1}\right)} + A_2 e^{\left(\frac{-x}{\tau 2}\right)} \quad (9)$$

Eq. (9) comprises three terms, where I represents the luminescent intensity as function of time, I_0 is a background constant, A_1 and A_2 are constants, τ_1 and τ_2 are the approximate characteristic lifetime decays of the OSL process. In Figs. 9(b) and 10(b), the main components of the fitted OSL curves for the glasses are shown.

For $PbO:H_3BO_3$, the fitted curve indicates two components with lifetimes of 0.9 s and 19.6 s. In the case of $PbO:H_3BO_3$-Al_2O_3, these values are 0.74 s and 20.3 s. The first exponential is related to a fast component, which is assigned to the electrons that recombine directly with the holes. The second exponential term relates to a slow component, due to the presence of shallow traps in the structure, where electrons are re-trapped for several seconds before being recombined with holes (Marini et al., 2015; Yukihara et al., 2017; D'amorim et al., 2014; Souza et al., 2017, 2014).

Fig. 11 shows the OSL dose response curve of the glasses. In the graphs, each point corresponds to the average response of 5 samples to a given dose. The experimental standard deviations are represented by error bars, barely visible, showing that the behavior of these samples is very reproducible. The OSL dose response curve presented a better fitting for a cubic polynomial equation, with chi-square of 0.994, as seen in Fig. 11(a). With the superlinearity index g (D) shown in Fig. 11(b) it is possible to see quantitatively how the dose response deviates from linearity. For $PbO:H_3BO_3$-Al_2O_3 a linear range can be observed from 0.5 to 2 Gy; above 2 Gy it is marked by a slightly sublinear region (< 6%) until 30 Gy; and above this value, a supralinear region is seen. The OSL dose response from $PbO:H_3BO_3$ is marked by a sublinear behavior from 0.5 to 30 Gy, and for higher absorbed doses, the OSL response is supralinear.

3.2.3. OSL/TL correlation

In Fig. 12(a) and (b) a comparison between the TL curve of $PbO:H_3BO_3$ and $PbO:H_3BO_3$-Al_2O_3 samples irradiated (no OSL bleaching) and the TL curves after irradiation and OSL bleaching is shown. As can be seen in Fig. 3(a), the TL emission peak of $PbO:H_3BO_3$ sample is composed by one TL emission peak located at 180 °C and two others, at 257 and 330 °C, which overlap in most of the doses. For $PbO:H_3BO_3$-Al_2O_3 sample, the glow curve is decomposed in three TL peaks (155 °C, 220 °C and 293 °C). Fig. 12(a) and (b) show that the optical stimulation bleaches preferentially the high–temperature TL peaks, leaving the low temperature TL peaks almost intact, which can be seen in the insets of Fig. 12(a) and (b). Thus, it is possible to conclude that the traps responsible for the TL peaks located at higher temperatures are probably those which contribute most to the OSL signal during optical stimulation of the samples. Therefore, the shallow traps responsible for the TL emission peaks at 180 °C and 155 °C of the $PbO:H_3BO_3$ and $PbO:H_3BO_3$-Al_2O_3 samples, respectively, do not have a significant contribution to the OSL signal.

4. Conclusion

In the present work, some important features of lead borate glasses ($PbO:H_3BO_3$ and $PbO:H_3BO_3$-Al_2O_3) were discussed for TL and OSL dosimetry, and as a complement, some structural characteristics of these materials were presented through the XRD and FT-IR analyses. As expected, the XRD results showed that these glasses present amorphous structure. From FT-IR results, it was observed that both glasses are composed of BO_4 units that are related to boron–oxygen rings; besides that, $PbO:H_3BO_3$-Al_2O_3 is also composed by BO_3 units.

From the TL point of view, it was observed that the $PbO:H_3BO_3$ samples exhibit glow curves with three TL emission peaks at 188 °C, 257 °C and 330 °C, while the TL emission of $PbO:H_3BO_3$-Al_2O_3 samples is composed by peaks around 155 °C, 220 °C and 293 °C. The latest TL peaks of these both materials have characteristics of dosimetric peaks. The kinetic parameters indicated that the TL glow curves do not fit neither first nor the second– kinetics order, being of general order. The values of *E*, *b* and *s* obtained from CFM and PSM methods are in very good agreement.

Results of OSL analyses indicated that the fitted decay curves of the glasses have two components, which are connected with a fast component and a slow component, respectively. Establishing a TL/OSL correlation between the results obtained by these two techniques, and considering that the optical stimulation preferentially bleaches the high–temperature TL peaks, it was concluded that the traps responsible for such peaks are the ones that contribute to OSL signal during optical stimulation of the samples.

This study brought an initial characterization of two new materials for ionizing radiation detection applications. Through the super-linearity index it was observed that the TL dose response from both glasses are linear in the range from 0.1 Gy to 4 Gy. For OSL, the linearity range is reduced to 0.5–2 Gy for the $PbO:H_3BO_3$-Al_2O_3, and the $PbO:H_3BO_3$ dose response can be observed from 0.5 Gy to 30 Gy, followed by a supralinear behavior. Although the sublinearity can be adjusted using correction factors, when the materials are applied for radiation dosimetry this possibility must be analyzed carefully, to avoid further errors in the estimation of the absorbed dose. Considering these first analyses, the TL technique is the most appropriate radiation dosimetry application for both studied glasses.

Acknowledgments

The authors gratefully acknowledge the support received of the Brazilian agencies CAPES and CNPq (Process 301335/2016-8 and 308090/20160).

References

Ahmed, M.F., Eller, S.A., Schnell, E., Ahmad, S., Akselrod, M.S., Hanson, O.D., Yukihara, E.G., 2014. Development of a 2D dosimetry system based on the optically stimulated luminescence of Al_2O_3. Radiat. Meas. 71, 187–192.
Akselrod, M.S., Akselrod, A.E., 2006. New Al_2O_3:C,Mg crystals for radiophotoluminescent dosimetry and optical imaging. Radiat. Prot. Dosim. 119, 218–221.
Akselrod, M.S., Botter-Jensen, L., Mckeever, S.W.S., 2007. Optically stimulated luminescence and its use in medical dosimetry. Radiat. Meas. 41, S78–S99.
Bhatt, B.C., Kulkarni, M.S., 2013. Worldwide status of personnel monitoring using thermoluminescent (TL), Optically stimulated luminescent (OSL) and radiophotoluminescent (RPL) dosimeters. Int. J. Lumin. Appl. 3, 6–10.
Bos, A.J.J., 2001. High sensitivity thermoluminescence dosimetry. Nucl. Instrum. Methods 184, 3–28.
Boulos, E.N., Kreidl, N.J., 1971. Structure and properties of silver borate glasses. J. Am. Ceram. Soc. 54, 368–373.
Chen, R., Mckeever, S.W.S., 1997. Theory of Thermoluminescence and Related Phenomena. World Scientific, New Jersey.
Cheng, Y., Xiao, H., W, G., 2007. Structure and crystallization kinetics of PbO–B2O3 glasses. Ceram. Int. 33, 1341–1347.
Chung, M.P., 2010. Handbook on Borates: Chemistry, Production, and Applications. Nova Science Publishers, New York.
D'amorim, R.A.P.O., Vasconcelos, D.A.A., Barros, V.S.M., Khoury, H.J., Souza, S.O., 2014. Characterization of α-spodumene to OSL dosimetry. Radiat. Phys. Chem. 95, 141–144.
Dayanand, M.S., 2004. Thermal (DSC) characterization of $xPbO–(1- x)P_2O_5$ glass system. Ceram. Int. 30, 1731–1735.
Doweidar, H., El-Damrawi, G., Mansour, E., Fetouh, R.E., 2012. Structural role of MgO and PbO in $MgO–PbO–B_2O_3$ glasses as revealed by FTIR; a new approach. J. Non-Cryst. Solids 358, 941–946.
El-Adawy, A., Khaled, N.E., El-Sersy, A.R., Hussein, A., Donya, H., 2010. TL dosimetric properties of $Li_2O–B_2O_3$ glasses for gamma dosimetry. Appl. Radiat. Isot. 68, 1132–1136.
Hirao, K., Mitsuyo, T., Si, J., Qiu, J., 2001. Active Glass for Photonic Devices: Photoinduced Structures and Their Application. Springer, Heidelberg.
Horowitz, Y.S., 1984. Thermoluminescence and Thermoluminescent Dosimetry, vol. 1, Beersheva [s.n.].
Hsu, S.M., Yang, H.W., Huang, D.Y.C., Hsu, W.L., Lu, C.C., Chen, W.L., 2008. Development and physical characteristics of a novel compound radiophotoluminescent glass dosimeter. Radiat. Meas. 43, 538–541.
Justus, B.L., Tommy, L.J., Alan, L.H., 1995. Radiation dosimetry using thermoluminescence of semiconductor-doped Vycor glass. Nucl. Instrum. Methods B 95, 533–536.
Kitis, G., Furetta, C., Prokic, M., Prokic, V., 2000. Kinetic parameters of some tissue equivalent thermoluminescence materials. J. Phys. D: Appl. Phys. 33, 1252.
Marini, A., Valença, J.V.B., Passos, R.A., Souza, S.O., Ciolini, R., d'errico, F., 2015. Production and characterization of $H_3BO_3–Li_2CO_3–K_2CO_3–MgO$ glass. Radiat. Phys. Chem. 116, 92–94.
Mckeever, S.W.S., 1985. Thermoluminescence of Solids. Cambridge Solid State Science Series, Cambridge.
Mckeever, S.W.S., Chen, R., 1997. Luminescence models. Radiat. Meas. 27, 625–661.
Mckeever, S.W.S., Yukihara, E.G., 2008. Optically stimulated luminescence (OSL) dosimetry in medicine. Phys. Med. Biol. 53, 351–379.
Mckeever, S.W.S., Moscovitch, M., Townsend, P.D., 1995. Thermoluminescent Dosimetry Materials: Properties and Uses. Nuclear Technology Publishing, Kent.
Pagonis, V., Kitis, G., Furetta, C., 2006. Numerical and Practical Exercises in Thermoluminescence. Springer Science & Business Media [SI].
Rao, D.R., Baskaran, G.S., Kumar, V.R., Veeraiah, N., 2013. Influence of sesquioxides on fluorescence emission of Yb^{3+} ions in $PbO–PbF_2–B_2O_3$ glass system. . J. Non-Cryst. Solids 378, 265–272.
Rao, M.S., Gandhi, Y., Sanyal, B., Bhargavi, K., Piasecki, M., Veeraiah, N., 2014. Studies on γ-ray induced structural changes in Nd^{3+} doped lead alumino silicate glasses by means of thermoluminescence for dosimetric applications in high dose ranges. J. Alloy. Compd. 616, 257–262.
Singh, N., Singh, Kanwar Jit, Singh, Kulwant, Singh, Harvinder, 2004. Comparative study of lead borate and bismuth lead borate glass systems as gamma-radiation shieldingmaterials. Nucl. Instr. Methods Phys. Res. B 225, 305–309.
Souza, L.F., Vidal, R.M., Souza, S.O., Souza, D.N., 2014. Thermoluminescent dosimetric comparison for two different MgB_4O_7: Dy production routes. Radiat. Phys. Chem. 104, 100–103. http://dx.doi.org/10.1016/j.radphyschem.2014.04.036.
Souza, L.F., Antonio, P.L., Caldas, L.V., Souza, D.N., 2015. Neodymium as a magnesium tetraborate matrix dopant and its applicability in dosimetry and as a temperature sensor. Nucl. Instrum. Methods A 784, 9–13.
Souza, L.F., Silva, A.M.B., Antonio, P.L., Caldas, L.V.E., Souza, S.O., D'errico, F., Souza, D.N., 2017. Dosimetric properties of MgB_4O_7:Dy,Li and MgB_4O_7:Ce,Li for optically stimulated luminescence applications. Radiat. Meas. http://dx.doi.org/10.1016/j.radmeas.2017.02.009.
Teixeira, M.I., Da Costa, Z.M., Da Costa, C.R., Pontuschka, W.M., Caldas, L.V., 2008. Study of the gamma radiation response of watch glasses. Radiat. Meas. 43, 480–482.
Yoshimura, E.M., Yukihara, E.G., 2006. Optically stimulated luminescence: searching for new dosimetric materials. Nucl. Instrum. Methods B 250, 337–341.
Yukihara, E.G., Mckeever, S.W.S., 2011. Optically Stimulated Luminescence, Fundamentals and Applications. John Wiley & Sons Ltd, London.
Yukihara, E.G., Whitley, V.H., Mckeever, S.W.S., Akselrod, A.E., Akselrod, M.S., 2004. Effect of high-dose irradiation on the optically stimulated luminescence of Al_2O_3:C. Radiat. Meas. 38, 317–330.
Yukihara, E.G., Doull, B.A., Gustafson, T., Oliveira, L.C., Kurt, K., Milliken, E.D., 2017. Optically stimulated luminescence of MgB_4O_7:Ce,Li for gamma and neutron dosimetry. J. Lumin 183, 525–532.
Yutaka, F., Yanagida, T., Futam, Y., Masai, H., 2014. Fluorescence and radiation response properties of Ce^{3+}-doped $CaO–Al_2O_3–B_2O_3$ glass. Jpn. J. Appl. Phys. 53 (05FK05).